Journal of Statistical Physics, Vol. 36, Nos. 5/6, 1984

Scaling Behavior of Surface Irregularity in the Molecular Domain: From Adsorption Studies to Fractal Catalysts

Peter Pfeifer,[1] David Avnir,[2] and Dina Farin[2]

For an unexpected variety of solids, the surface topography from a few up to as many as a thousand angstroms is very well described by fractal dimension, D. This follows from measurements of the number of molecules in surface monolayers, as function of adsorbate or adsorbent particle size. As an illustration, we present a first case, amorphous silica gel, where D has been measured independently by each of the two methods. (The agreement, 3.02 ± 0.06 and 3.04 ± 0.05, is excellent, and the result is modeled by a "heavy" generalized Menger sponge.) The examples as a whole divide into amorphous and crystalline materials, but presumably all of them are to be modeled as random fractal surfaces. The observed D values exhaust the whole range between 2 and 3, suggesting that there are a number of different mechanisms by which such statistically self-similar surfaces form. We show that fractal surface dimension entails interfacial power laws much beyond what is the source of these D values. Examples are reactive scattering events when neutrons of variable flux pass the surface (this is of interest for locating fractal substrates that may support adlayer phase transitions); the rate of diffusion-controlled chemical reactions at fractal surfaces; and the fractal implementation of the traditional idea that the active sites of a catalyst are edge and apex sites on the surface.

KEY WORDS: Solid surfaces; fractal structures; adsorption; neutron scattering; interfacial diffusion; catalysis.

1. EXPERIMENTAL ACCESSIBILITY OF MOLECULAR FRACTALS

This paper reports on advances in recent investigations[1-7] of fractal properties of solid surfaces at the molecular range, particulars being the

[1] Fakultät für Chemie, Universität Bielefeld, D-4800 Bielefeld, West Germany.
[2] Department of Organic Chemistry, The Hebrew University of Jerusalem, Jerusalem 91904, Israel.

0022-4715/84/0900-0699$03.50/0

corroboration of the analytical method and some exemplary applications. To set the stage, we first clarify how the subject relates to other instances of fractal structures (of which a host indeed has accumulated in the past few years).

It seems fair to say that macroscopic nature is a rich source of direct experimental evidence of fractal objects, but has furnished clues as to the underlying mechanisms only in few cases so far—while in the microscopic (molecular) regime, most fractral structures known to date have entered the picture through theoretical work, and tend to be observable only by comparably indirect methods. Indeed: The experimental paradigms for fractals are landscapes[8] and the like,[9] turbulence[8,10] (also clouds[11] and sea surface[12]), electric discharges,[13] biological structures ranging from cauliflower to tissues,[14] rings of Saturn,[15] and mass distribution in the universe.[8] While the prominent examples from theory are critical fluctuations in phase transitions,[16] infinite clusters in percolation,[17] self-avoiding random walks[18] and other polymer models,[19] diffusion-limited aggregation and relatives,[20] commensurate–incommensurate phase transitions (for a review see Ref. 21), wave functions and density of states in quasiperiodic potentials,[22] chaotic attractors and all that (for an overview see Ref. 23). One reason why many of these self-similar structures in the molecular domain are not amenable to straightforward observation, is that they typically refer to dynamical aspects and hence cannot be studied by inspection similar to the inspection of a macroscopic fractal (in the strange-attractor case, the fractal even lives in a space different from configuration space). And if they do refer to a "frozen" situation such as in percolation, their geometric scaling properties are characteristically inferred from measurements of electrical conductivity, magnetic susceptibility, or elastic moduli (for gels).[3]

Are there, then, any microscopic fractals that can be measured, and assessed, with equal conceptual simplicity[4] as the mentioned macroscopic cases? The surfaces to be discussed in this paper are of this type. Other than that, the list (ordered by ascending inner cutoff, i.e., length scale below which the fractal behavior subsides) is short as yet: Analysis of atomic positions has shown various proteins to have fractal backbones in the crystalline state.[24] By determination of fractal dimension from electron micrographs, discontinuous thin metal films[25] and aggregates of fume silica (this follows from data presented in Ref. 26) and of gold colloids[27] have been identified as percolation clusters and diffusion-limited aggregates, respectively. Finally,

[3] Note also that some of these quantities are monitored jointly by fractal and spectral (fracton) dimension, and so may not yield separate information about the two. See contributions of these proceedings.

[4] For example, from length–yardstick or mass–radius relations (Ref. 8).

at the margin of the molecular domain (i.e., at inner cutoffs of about 10^3 Å) and beyond, fractal dimension of particle contours, e.g., of crystal agglomerates, has been measured from micrographs.[28] Note that all items except the last correspond to fractal curves (some highly branched) rather than to surfaces.

Thus, the class of surfaces in question fills some gaps as follows:

(i) Inner cutoffs are really at atomic distances, typically at a few angstroms.

(ii) Fractal surface dimension and fractal curve dimension may coincide (if the curve is sufficiently space filling), but the topological differences between the two substrate classes promise interesting variations in the physics on them.[16,29] [Note that some of our examples carry an extensive system of *through*-pores (channels, holes) similar to a Menger-type sponge[8] with finite inner cutoff, in which case the fractal idealization will after all amount to a spatial, infinitely ramified curve.] Such physics is promoted by the corollary of direct observability, that the fractal can be nondestructively "seen" by external probes like photons, molecules, etc.

(iii) The surface topography at molecular scales of solids is decisive in adsorption phenomena (e.g., ordered phases of adlayers), corrosion, electrochemistry in general, catalysis, and microelectronics, to name a few. Prior to fractals, there has been little guidance to an effective characterization of the issue of roughness in any of these fields.[6]

(iv) While some metal surfaces do resemble downscaled terrestrial landscapes (for a review see Ref. 30) and may perhaps be modeled as fractional Brownian reliefs,[8] many of our case studies beg for *porous* random fractals as models.

2. THE BASIC POWER LAWS

Unless particularly prepared (e.g., sputtered and annealed metal crystals, exfoliated graphite, some fume silicas), solids tend to have a microscopic surface structure that cannot be reasonably described in terms of height above some standard reference manifold (plane, sphere,...). This type of situation, originating from absence of globally directive forces (like gravity in geomorphology), is referred to as porosity. It has two important consequences: First, since much of the surface is hidden with respect to any straight-line path in a beam of incoming projectiles, only *X*-rays and neutrons (for which most substrates are practically transparent), or diffusing molecules can effectively probe all of the relevant surface. This delineates some of the experimental techniques at our disposal. Second, even if an atlas of maps of the surface were available, Fourier methods are not applicable for

the analysis (but see also Ref. 6). This prepares us for looking for other data than variances of increments.[9]

These remarks suggest the following quite general procedure to study surface irregularity in the molecular domain: Adsorb a monolayer of identical molecules, each of effective cross-section area σ, on the surface and count their number. Usually this number is expressed as number of moles, n, per gram of adsorbent (see also below). If then we go from large to small molecules (yardsticks) for adsorption, surface features comparable in size manifest themselves by a growth of n faster than const $\cdot \sigma^{-1}$. Specifically, if the cross sections of the different molecules are geometrically similar and

$$n \propto \sigma^{-D/2} \tag{1}$$

holds with $D > 2$ (for $\sigma_{\min} \leqslant \sigma \leqslant \sigma_{\max}$), the surface has the fractal dimension D (over the yardstick range $[\sigma_{\min}, \sigma_{\max}]$). Before we proceed to examples for (1), several remarks are in order:

(a) For spherical molecules, with radii r, Eq. (1) reduces to $n \propto r^{-D}$. This is the definition of fractal dimension.[8] (Indeed, it is equivalent to that const $\cdot r^{-D}$ balls of radius r, $r \to 0$, are required to envelop the object, here the surface, by inclusion. Since the surface can fill no more than a volume, one has $2 \leqslant D < 3$ altogether.)

(b) Being the surface analog of the coastline-of-Britain analysis,[8] Eq. (1) asserts microscopic surface fractality as directly as any of those studies. It does so without the restriction to isotropic surfaces inherent in other approaches.[9,28],[5]

(c) Standard methods exist to measure n and σ. The mole numbers n result from adsorption isotherms.[31] In the simplest case (Langmuir isotherm), the amount adsorbed approaches a constant value with increasing equilibrium pressure or concentration of the species to be adsorbed, and n is this value. The area σ occupied by a single molecule obtains from molecular models, monolayers on flat surfaces, liquid molar volume v of the compound to be adsorbed, or radii of gyration (when yardsticks are polymers).[3,4] For instance, for suitable adsorbate series one has $\sigma \propto v^{2/3}$, which turns (1) into a relation between macroscopic quantities alone, $n \propto v^{-D/3}$. (Note: Customarily, measured values for n and σ are converted into specific surface area, Avogadro's number $\times n\sigma$. To avoid the problem that this may be a poor invariant, it has become standard to use nitrogen as reference yardstick. In as far as nitrogen is among the smallest available yardsticks, according surface areas like 10^3 m^2/g for silica gel or activated carbon may then be read as the practitioner's version of infinite surface area of a corresponding fractal model.)

[5] For Fourier-analytic options see Ref. 6.

(d) In all examples to date, both for (1) and Eqs. (2)–(3) below, σ_{min} and σ_{max} reflect limited available data, not any observed departure (crossover) from the power law in question. That is, our yardstick ranges only imply that

$$\text{inner cutoff} < (\sigma_{min})^{1/2}$$

$$\text{outer cutoff} > (\sigma_{max})^{1/2}$$

the actual cutoffs for fractal behavior remaining unexplored. In particular, σ_{min} and σ_{max} comfortably satisfy the condition of "minimal self-similarity" (or exclusion of nonrecurrent irregularities), $\sigma_{max}/\sigma_{min} \gtrsim 2$.[6]

(e) The condition that the yardstick molecules be similar to one another cannot be relaxed very much (only for a smooth surface, $D = 2$, is it redundant). Indeed, if the molecules are rods of variable length and constant width, parallel aligned on an isotropic surface, Eq. (1) has to be replaced by[3]

$$n \propto \sigma^{-D+1} \tag{2}$$

Such variations of functional dependence can be used to discriminate between competing adsorbate geometries, in special cases even without prior knowledge of D.[3,4]

Examples for surfaces with well-defined dimension greater than 2, determined from Eq. (1) or variants thereof, borrow from quite varied materials (D and the yardstick range, in Å^2, are given in parentheses): Graphite (2.07 ± 0.01, 16–178)[4]; carbon black (2.25 ± 0.09, 16–71)[4]; activated carbon (2.30 ± 0.07, 16–47)[4]; porous alumina (2.79 ± 0.03, 16–451000)[5]; porous silica gel (2.94 ± 0.04, 16–34).[1] This is just a selection from Refs. 4 and 5 [there and in Refs. 1, 6, 7, it is literature data that has been analyzed in terms of Eqs. (1)–(3)]. For instance, the activated carbon is a member of a series in which activation-controlled smoothening of micropores is observed as progression of D values all the way from 3 to 2; and alumina is one out of three cases where polymers serve as yardsticks.

Here, however, we wish to present results of experiments[32] designed to show (for the first time) that fractal behavior determined from Eq. (1) is perfectly recovered by other methods, here Eq. (3). So the natural place to discuss this most recent example for (1), is following the results (3)–(5) which we now introduce.

Apart from polymer adsorption, n vs. σ measurements for molecules much larger than, say, C_{10} species, are exceptional (also in difficulty). This is the background of some narrow yardstick ranges in above examples for

(1), and is where another relation steps in—one that allows considerably larger yardstick ranges to be scanned effectively. It is geared to particulate adsorbents and states that, for a *fixed* reference adsorbate (usually nitrogen) and geometrically similar adsorbent particles of variable diameter $2R$, the monolayer mole number n varies according to

$$n \propto R^{D-3} \tag{3}$$

the amount of adsorbent being held constant by volume ($\gg R^3$). The according experimental procedure is quite similar to that for (1), except that we now vary particle (substrate) rather than yardstick size. In fact, Eqs. (1) and (3) can be derived from each other[3] by noting that upscaling of the yardstick from $\sigma_{\min}$ to σ, on a surface of diameter $2R_{\max}$ [Eq. (1)], is equivalent to downscaling of the surface from $2R_{\max}$ to $2R = 2R_{\max}(\sigma_{\min}/\sigma)^{1/2}$, under the yardstick of area $\sigma_{\min}$ [Eq. (3)]; and that the factor R^{-3} in (3) accounts for the number of such particles contained in a macroscopic volume. Of course, the power law (3) is simply a variant of the area–volume relation[8] for a fractal surface, but the preceding argument has the virtue of yielding also the important interconversion of yardstick and particle ranges. It is contained in the following equivalence[3]:

$$\left.\begin{array}{l}\text{(1) holds for } \sigma_{\min} \leqslant \sigma \leqslant \sigma_{\max} \\ \text{and particle diameter } 2R_{\max}\end{array}\right\} \Leftrightarrow \left\{\begin{array}{l}\text{(3) holds for } R_{\min} \leqslant R \leqslant R_{\max} \\ \text{and yardstick area } \sigma_{\min}\end{array}\right. \tag{4}$$

where

$$\frac{R_{\max}}{R_{\min}} = \left(\frac{\sigma_{\max}}{\sigma_{\min}}\right)^{1/2} \tag{5}$$

The asymmetry in (4), i.e., that $\sigma_{\min}$ and $R_{\max}$ are preferred over, e.g., $\sigma_{\max}$ and $R_{\min}$, is dictated if the particles are only required to be similar to each other within the resolution given by the reference yardstick for (3). In practice such approximate similarity is often granted by a common origin of the particles,[3,6] and may even be dispensed with on the grounds that it is highly unlikely that a sequence of completely unrelated particle shapes should satisfy Eq. (3) ("maximum-likelihood estimation").[7] Finally, note that possible particle agglomeration cannot alter Eq. (3) in any significant way.[6]

Examples for D values and yardstick ranges determined from Eqs. (3)–(5), are even more numerous than those from (1).[4–7] Many of them are crystalline: quartz (2.15 ± 0.06, 16–10 600)[5,7]; calcite (2.16 ± 0.04,

[6] It also conforms with the "principle of least-biased guess" (Jaynes).

[7] By the same token, one may also weaken *yardstick* similarity for Eq. (1).

20–47000)[5,7]; α-Fe00H (2.57 ± 0.04, 16–980)[5,7]; dolomites of different origins (2.58 ± 0.01, 2.91 ± 0.02, 20–47000)[5,7]; kaolinite (2.92 ± 0.01, 150–16500).[5–7]

Thus, as a rule from (1) and (3), one has that observed D values fall anywhere between 2 and 3; that standard deviations are around 0.05 and compare very well with those from simulation[33] on models with well-defined D by construction; and that $\sigma_{max}/\sigma_{min}$ ratios within easy reach are $\lesssim 10$ for Eq. (1) (recall alumina, however), and $\sim 10^3$ for Eq. (3).

3. POROUS SILICA GEL, REVISITED

The announced experimental confirmation that the power laws (1) and (3) yield the same value for fractal dimension was carried out on porous silica gel (Woelm). So the surface is a close relative (but of a different producer) of the adsorbent analyzed in Ref. 1, and we can draw on some facts from there: (i) The result $D = 2.94$ (see preceding section) suggests that we should find a dimension as strikingly off the classical value of two. (ii) Suitable adsorbates are aliphatic alcohols. They attach to the surface by hydrogen bonding of the alcoholic OH group to a surface OH group, and thus form monolayers well identifiable from Langmuir isotherms. (iii) Cross sections σ can be monitored by varying the alkyl group of the alcohols.

In the experiments here, alcohols were adsorbed from toluene solution. As expected for such nonpolar solvent, all monolayer values n could be read off from perfect (straight-line) Langmuir plots.[31] Underlying the n vs. σ analysis [Eq. (1)] were identical substrate samples, each with particle diameters in the range 63–200 μm (with the same distribution of course). The yardsticks were methanol, ethanol, isopropanol, tertiary butanol, and tertiary amyl alcohol, i.e., a series of *spherical* alcohols. This choice not only meets the condition of geometrically similar yardsticks in the simplest possible way, but also furnishes unambiguous σ values from liquid density of the respective alcohols.[8] The results, n and σ, are shown in Fig. 1. They obey the anticipated scaling, Eq. (1), with $D = 3.02 \pm 0.06$ and yardstick range 18–35 Å^2.

On the other hand, the substrate samples for the n vs. R analysis [Eq. (3)], each homogeneous with respect to particle size, were prepared by sieving of the source material. The reference yardstick chosen was tertiary amyl alcohol, the largest of the yardsticks used in the n vs. σ analysis. The resulting n and R values (Fig. 2) satisfy Eq. (3) with $D = 3.04 \pm 0.05$, the screened range of particle diameters being 71–192 μm. By (4) and (5), this implies (1), with $D = 3.04 \pm 0.05$, over the yardstick range of 35–256 Å^2.

[8] The model assumptions underlying this standard conversion of molar volume into molecular cross sections are recalled in Ref. 3.

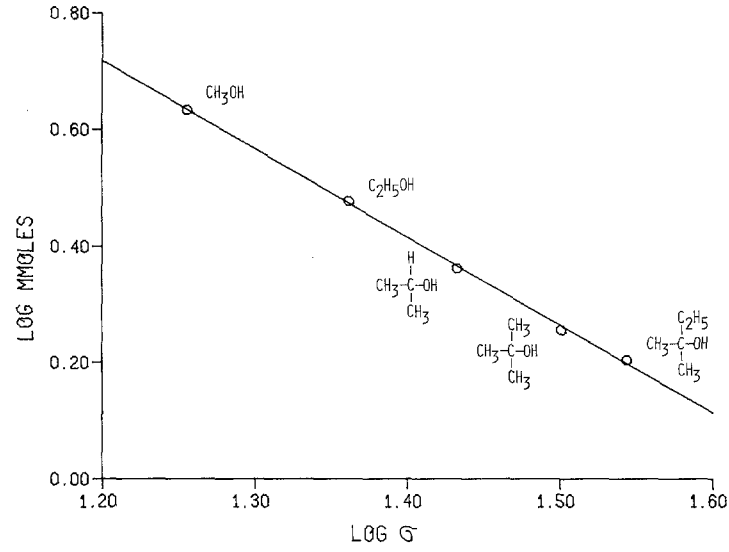

Fig. 1. Measured monolayer mole numbers n as function of cross section σ (Å^2) of adsorbate molecules. The resulting dimension, from Eq. (1), is $D = 3.02 \pm 0.06$.

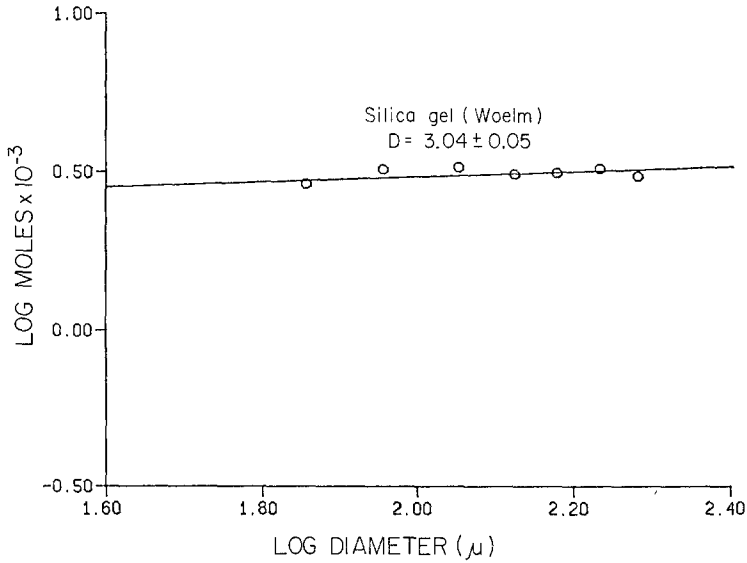

Fig. 2. Measured monolayer mole numbers n of tertiary amyl alcohol as function of adsorbent particle diameter $2R$ (μm). From Eq. (3) there results the indicated D value.

Thus the two modes of analysis, complementary as they are, yield the same result (within standard deviations, one is the analytic continuation of the other). This is an important benchmark for the valuation of the two methods, and hence of previous surface dimensions.

There are several ways of appreciating the extreme situation that a surface, here of silica gel, has dimension virtually 3:

(a) The surface is so crumpled and porous that there is no gain in effective surface area when a fixed volume of adsorbent particles of given size is replaced by the same volume of similar, but much smaller particles. This is the meaning of Eq. (3) for $D = 3$ (for an illustration, see Ref. 7). It follows, e.g., that surface contributions[34] to thermodynamic properties of the solid are no longer negligible compared to bulk contributions. Indeed, the right-hand side of (3) is also the effective surface area per unit volume for a single particle, so that for $D = 3$ the ratio of the two contributions ceases to go to zero with increasing size of the system, R.

(b) Equation (1) for $D \lesssim 3$ reflects that the surface is space filling to a degree that a monolayer amounts to a bulk phase interrupted by few small, and an increasing number of ever smaller, voids. (There are voids that correspond to pores through which the adsorbed molecules have entered; and "voids" that correspond to the support of the monolayer, including pores too small to be accessible to the molecules under consideration.) This cascade of diminishing voids renders silica gel quite distinct from a zeolite, which also has a pore structure permeating everywhere, but one that is a periodic array of (intersecting) channels of uniform width. Indeed, silica gel has no molecular-sieve properties characteristic of zeolites.

(c) An *a priori* fractal model for silica gel suggests itself as follows. Micrographs of spongy materials often exhibit a surprisingly smooth looking surface, punctured by appreciable pore entrances only here and there, the largest of these pore widths, $2\rho_{\max}$, being considerably smaller than the particle diameter, $2R_0$. As the resolution is increased by a factor M, smaller pores become visible of course, but the number of those with diameter $\sim 2\rho_{\max}/M$ in the field of vision remains low. This state of affairs can be mimicked by a "heavy" generalized Menger sponge with $b \sim R_0/\rho_{\max}$: There,[8] a unit cube is divided into b^3 cubes of length $1/b$ (generally, b is a fixed, odd integer $\geqslant 3$), and in a first step $3(b-1)+1$ of these cubes are removed so that the original cube becomes punctured by three channels of width $1/b$ that intersect in the cube's center at right angles. In each of the remaining cubes of side $1/b$, similar channels of width $1/b^2$ are then introduced; etc. There results a fractal sponge with dimension

$$D = \log(b^3 - 3b + 2)/\log b$$

Thus, even the conservative estimate $b = 7$ predicts a surface dimension as high as $D = 2.97...$ for silica gel. A refinement of the model might distribute the pore volume created at every stage among more than three channels per cube (cf. also the carpet constructions in Ref. 35). Such yields a fractal of lower lacunarity,[8,35] but the dimension remains unchanged. In particular, any of these models retrieves the datum that virtually all surface of silica gel is internal, and that most entrances from outside are invisible to any electron microscope.

4. CROFTON'S THEOREM AS SCATTERING EXPERIMENT

This section describes further, geometric consequences of molecular surface fractality (see Section 5 for explicitly dynamical, time-dependent ones). Such scaling properties other than (1)–(3) enlarge the possibilities of experimental analysis of fractal structures and are the source of various applications. The scattering experiment to be proposed is one of them and implements the alternative, indicated in Section 2, to surface probing by diffusing molecules.

For an illustration of applications, we transplant the mass–radius relation[8] and the diameter–number relation[8] [general, *ab initio* derivations of (6) and (7) are given in Ref. 3]. Geared to surface problems these relations assert that if the surface has dimension D, the number N of adsorption sites (for molecules of a given kind) within distance l from any fixed site obeys

$$N \propto l^D \tag{6}$$

and the total volume V of pores of diameter $\geqslant 2\rho$ obeys

$$-\frac{dV}{d\rho} \propto \rho^{2-D} \tag{7}$$

Equation (6) mediates between the radial density of molecules in a plane ($D = 2$) and that in a volume ($D = 3$), and hence is a measure of effective interactions (mean field, etc.) between admolecules on a D-dimensional surface. This of course bears on phase transitions in adlayers.[3,16,35] Result (7) is the fractal answer to the problem of determining the pore-size distribution which governs numerous transport processes.[36] Inasfar as Eq. (7) is implied by any[6] experimental finding of (1) or (3), it is perhaps the first experimental pore-size distribution that is free of the ambiguity that the traditional experimental data[31] can be interpreted in terms of vastly different pore-size distributions.[37] [Note that (7) holds even for porous structures with $D < 2$, such as "light" generalized Menger sponges.[8] Note

also that both in (6) and (7) the proportionality factor is independent of the size of the surface. Rather, it is a measure of lacunarity.[8]]

Of particular interest are methods of experimental analysis that can follow the fractal behavior established by (1) or (3) to still larger scales. For example, in order for a surface to support an adlayer phase transition in $2 < D < 3$ dimensions, the yardstick range for (1) should be something like 10^1–10^6 Å^2 or more. Such $\sigma_{\max} \gtrsim 10^6$ Å^2 is well in the domain of electron microscopy, and one may check up on D by image analysis.[28] For exceptional spheroidal or pseudoplanar surfaces, surface profiles may even be representable as single-valued function ("altitude") of angle or rectilinear coordinate, respectively, in which case well-developed instrumental methods of Fourier analysis can serve to measure D (for isotropic surfaces)[6]: If the kth coefficient in the expansion of the altitude-angle function scales with k like $k^{-\alpha}$, or if the power spectrum of altitude vs. horizontal locus decays like $\omega^{-\beta}$ for increasing frequencies ω, then

$$D = \max\{2, 3 - \alpha\} \tag{8a}$$

and

$$D = \max\left\{2, \frac{7 - \beta}{2}\right\} \tag{8b}$$

respectively.

In contrast, the method we shall now set forth is neither conditioned to visible surface features, nor does it necessitate large-scale fractal behavior to be put together from different analyses [say, from (1), (3), and (8)]. It counts reactive collision events when particles in a suitable beam strike the surface. Thus, it also contrasts with elastic, all diffractive scattering at projectile wavelengths much larger than the inner cutoff of the fractal.[12,38]

The basic ingredient is Steinhaus's version of Crofton's theorem.[39] It states that the length of a curve in the plane, measured with yardsticks of length r, can be obtained as follows: Cover the curve with an array of equidistant parallels (separation r) and count the number of resulting intersections, S_1. Choose an integer m, rotate the grating around a fixed point in angular steps of π/m, and at each orientation count the respective number of intersections, $S_2, \ldots, S_m$. Then,

$$\lim_{m \to \infty} \frac{r\pi}{2m} (S_1 + \cdots + S_m) \tag{9}$$

is the length in question [specifically, (9) is a Riemann approximation of a *double* integral for the Jordan length of a rectifiable curve].

Similarly, the area of a surface, measured with squares of side r, obtains by intersecting the surface with an analogous, but spatial array of parallel straight lines (separation r) and averaging the number of intersections over all possible orientations: Apart from an universal factor, this average equals the number of squares of side r required to cover the surface. The point is that such intersections can be physically realized and counted by looking for specific events that signal the traversal of an incident particle through the surface, the substrate itself being transparent for the particles (so that points of exit and reentries along the straight-line trajectory are equally detectable). One way of doing this is to "paint" the surface with a Gd monolayer, to rotate the sample in a wide neutron beam of flux I, and to count the number N of γ quanta characteristic of the reaction

$$^{157}\mathrm{Gd} + n \rightarrow {}^{158}\mathrm{Gd}^* \rightarrow {}^{158}\mathrm{Gd} + \gamma$$

over a fixed interval of time. (Gd is chosen for its large capture cross section, resulting in an effective nuclear diameter of 0.05 Å.) Assuming the same neutron velocity at different fluxes, one has a mean separation r between trajectories in the beam proportional to $I^{-1/2}$ and, hence, that

$$N \propto I^{D/2} \tag{10}$$

for a surface of dimension D. The proviso is that the counting interval must be short enough that N remains a fraction of all Gd atoms on the surface (otherwise N would merely count the total number of Gd atoms).

In reality neutrons do not come in regularly spaced trajectories, of course; nor can a single neutron light up more than one Gd atom along its path. So a more detailed argument asserts that regularly and randomly spaced parallels of the same density are equivalent (in fact, Crofton's original result considers the expectation value of the number of intersections of a random line with the curve); and that incomplete counting of all entries and exits along a single path is balanced by the correspondingly higher capture probability along the path.

Finally, we mention that the Gd-painted surface might also be probed by a microbeam of neutrons (available from suitable diffraction). In that case, one counts N as function of beam diameter $2l$ (the flux is now kept constant) so as to observe the power law (6).

5. CATALYTIC ACTIVITY AND OTHER FRACTAL-INTERFACE KINETICS

Much of the eminent role of surfaces is due to their capability of controlling physical and chemical processes with respect to both pathways and rates. We focus here on interfacial processes, i.e., relating to transport to

and from (rather than on or along) the surface. Almost by definition then, the rate is proportional to the number of "active sites" on the surface. These sites may be the total of surface atoms (or other chemical units), energy-rich asperities (surface steps, dislocations, etc.), may be dictated by geometric accessibility (e.g., pores larger than the guest), or dynamic accessibility (first-passage time for migration to the surface). So one expects fractal surfaces to carry all kinds of dimension-dependent kinetics. This section explores some of it.

The mentioned proportionality between rate and number of active sites can well entail a nonlinear dependence of population on time, for example, if the number of active sites itself depends on time. An instance is interfacial diffusion for small times.[40] It is instructive to derive the result as application of Eq. (7): Consider diffusion of carriers of excitation (charge, spin polarization,...) from a fluid to a porous solid. Upon impinging on the surface they are to lose their activity (discharge, relaxation,...). Starting from a homogeneous population in the fluid at time 0, we want to estimate the number $Q(t)$ of carriers deactivated up to time t. For small t and diffusion coefficient $\mathscr{D}$, this amounts to all carriers within distance $\sim(\mathscr{D}t)^{1/2}$ from the surface,[40] i.e., those in pores of diameter $\leqslant 2(\mathscr{D}t)^{1/2}$ plus those in a layer of thickness $(\mathscr{D}t)^{1/2}$ lining the walls of pores of diameter $>2(\mathscr{D}t)^{1/2}$. Thus, $Q(t)$ is the number of carriers in the volume

$$\int_0^{(\mathscr{D}t)^{1/2}} \left(-\frac{dV}{d\rho}\right) d\rho + (\mathscr{D}t)^{1/2} \int_{(\mathscr{D}t)^{1/2}}^{\infty} \frac{2}{\rho} \left(-\frac{dV}{d\rho}\right) d\rho \tag{11}$$

where $-dV/d\rho$ is the pore-size distribution (cf. Section 4) and $2/\rho$ is the ratio of area to volume of an open cylinder of radius ρ (this pore shape is just for the sake of definiteness). Substitution of (7) into (11) yields

$$V_{\text{tot}} \left(1 + 2\frac{3-D}{D-2}\right) \left(\frac{\mathscr{D}t}{\rho_{\max}^2}\right)^{(3-D)/2} \tag{12}$$

where the proportionality factor in (7) has been expressed in terms of total pore volume V_{tot} and $\rho_{\max}$ by $V_{\text{tot}} = \int_0^{\rho_{\max}} (-dV/d\rho)\, d\rho$. Whence the desired result[40]

$$Q(t) \propto t^{(3-D)/2} \tag{13}$$

[for $(\mathscr{D}t)^{1/2} \ll$ outer cutoff]. Equation (12) shows that for $D \lesssim 3$ the fluid is depleted of all excitation (V_{tot}) almost instantaneously. Whereas for $D \to 2$ the depleted volume (12) goes to zero [one can show that the prefactor in (7), here written as $(3-D)V_{\text{tot}}\rho_{\max}^{D-3}$, vanishes faster than $(D-2)^{3/2}$ for $D \to 2$], in accordance with the fact that (11) and (12) count only deac-

tivation at *internal* surface. If all surface is wanted instead, one uses Eq. (1) to replace the second integral in (11) by the total surface area measured with yardsticks of area $\mathscr{D}t$ which in (12) and (13) alters just the prefactors.

An application of (13) is that the conductance between an electrolyte and a solid electrode varies with the current frequency ω as $\omega^{(D-1)/2}$.[40] For experiments of this type, analyzed in fractal terms differently, see Ref. 41.

The result (13) bears also on any diffusion-controlled chemical reaction between a liquid and a solid: If the surface remains formally unchanged during the reaction ("catalysis"), then (13) describes the increase of product concentration $[\propto Q(t)]$ with time. The same is true if the reaction consumes the solid but preserves its shape. [Indeed, since the prefactor in (7) is independent of the surface size, shrinkage of the surface affects (13) only to the extent that, upon restriction of the integration in (11) to $\rho \leqslant \rho_{\max}$, there arises a size-dependent boundary term in (12); which, even for accordingly t-dependent $\rho_{\max}$, does not change (12) and (13) in leading order of t.] If the surface shape does change in the course of the reaction, e.g., by disappearance of successively larger pores, it does so in a manner such that, at the instant of consideration, fractality has subsided precisely up to length scales over which the liquid has been deactivated so far; i.e., the shape is preserved within lengths across which diffusion has yet to take place. So, again, the onset of the reaction obeys (13). More generally, (13) is universal because the surface's global property of being fractal can be undermined by diffusion-controlled reaction only on time scales outside the domain of (13). (Thus diffusion-controlled growth of fractal aggregates from nonfractal seeds[20] falls outside the present discussion.)

Reactions whose rate-determining step is not mass transport usually have a finite initial velocity [unlike (13)]. When the reaction occurs uniformly at all accessible surface sites, this velocity is proportional to the surface area measured with the reactant molecule as yardstick, and its measurement as function of particle size R of the solid yields the surface dimension through Eq. (3) with n replaced by initial velocity. An example is provided by the dissolution of quartz in hydrofluoric acid where such experimental data, for crushed quartz, implies[7] $D = 2.21 \pm 0.01$ [with $\rho_{\max}/\rho_{\min} = 495$ from (5)]. Note the agreement with the D value, from adsorption, for quartz of a different origin (Section 2).

For many catalytic reactions, however, the rate (usually expressed as activity of the catalyst, i.e., the amount of substance converted per unit mass of catalyst and unit time) is not governed by the whole of accessible surface sites. For instance, a catalyst may be fully deactivated by far less poison than what is required for monolayer coverage. (It remains to be explored whether, in some cases, such poisoning may also involve the inhibition of D-dimensional condensates.[3]) The time-honored idea is[42] that the reaction

proceeds only at energy-rich, active sites, often modeled as edge or apex sites (adlineation theory). A standard model is to assume the catalyst as consisting of cubic crystallites of side R (total volume fixed and $\gg R^3$) and that the activity, a, is proportional to total surface area, edge length, or number of corners. Then $a \propto R^{-1}$, R^{-2}, or R^{-3}, respectively. But in practice, power laws $a \propto R^{-v}$ with $v = 1, 2, 3$, or superpositions thereof, are much less common than those with $v < 1$ (for the case of supported metal catalysts, see, e.g., Ref. 43). We now sketch how fractal catalyst surfaces (for which alumina and silica gel in Sections 2 and 3 are examples) can account for such $v < 1$ in all respects. Consider for definiteness Menger's sponge[8] of side R and cover it with square molecules of side $r_0 \ll R$. The resulting monolayer has a well-defined surface area, edge length, and number of corners (for the sponge itself this distinction fails, in accordance with the sponge's being nowhere differentiable). Respective division by r_0^2, r_0^1, and r_0^0 defines the number of plane, edge, and corner sites (for resolution r_0). Each of these numbers grows with R as R^D, and it is easy to see that this is so for any self-similar surface. Thus, replacing the above cubic crystallites by fractal ones of surface dimension D, we obtain

$$a \propto R^{D-3} \tag{14}$$

where the active-site type enters through the prefactor. [While formally identical with (3), Eq. (14) rests on much more liberal hypotheses, corresponding to submonolayers of any degree of coverage. Hence also (3) holds under these weaker conditions.]

Can such fractal adlineation theory also explain empirical power laws $a \propto R^{-v}$ with noninteger $v > 1$? Yes, if we recognize that many metal surfaces show steps and terraces that do not lend themselves to a fractal-surface model, but rather to a fractal-step model (distinct from fractal-slope models for the sea surface[12]). Indeed, if for example the crystallites are prisms of height R with basal profile joined from four Cantor staircases[8] so that the end points of the staircases form a square of side R, then the number of plane, edge, and apex sites (for fixed resolution) on a single crystallite is proportional to R^2, $R^{1+D'}$, and $R^{D'}$, where $D' = \log 2/\log 3$ is the dimension of the set of nondifferentiability of the profile. Thus, multiplying by R^{-3}, one obtains edge-controlled and apex-controlled activity with respective exponent $1 < v < 2$ and $2 < v < 3$, as desired.

6. CONCLUSION

The relation of fractal surfaces of solids to other molecular fractals has been discussed from the viewpoint of direct experimental observability. It has

been shown that ubiquitous porosity does not obstruct such observability if the surface is suitably probed by adsorption or selective neutron (possibly also short-wave X-ray) scattering. The case presented here in some detail, silica gel, demonstrates this to an extreme (both porositywise and with regard to analysis by different experimental procedures). The corresponding model, a heavy Menger sponge, shows that dimensions virtually 3 should not be a surprise.

Viewing fractal surface geometry as statistical mechanics of surface irregularity (cf. also Ref. 6), one expects—and indeed finds—many distinguished implications of such irregularity (Sections 3–5). In fact, the exponents in the resulting power laws share all characteristics of critical exponents for phase transitions and other critical phenomena: Many of them describe, for $D > 2$, the divergence of an "ordinarily" well-defined quantity in some limit (e.g., surface area [cf. Eq. (1)]; the roughness factor, defined[31] as ratio of the surface area by nitrogen adsorption to the surface area by electron or optical microscopy [cf. Eq. (3)]; pore distribution [Eq. (7)]; deactivation per diffusion length [cf. Eq. (13)]). This is the analog of thermodynamic singularities for a phase transition. The analog of scaling laws and universality is that the exponents are not independent of each other but manifestly satisfy sum rules similar to those for critical exponents. Here universality says that the exponents depend only on the dimension of the surface, while the sum rules themselves are the same for all D.

Such parallels are due, of course, to the, respectively, underlying self-similarity (carried by the critical fluctuations, i.e., geometrically similar clusters of all sizes, for phase transitions). But they also suggest that fractal surfaces, as described here, themselves may be frozen, critical phenomena (recall Section 1 and that fracture of a solid can be understood as a critical phenomenon, too).

Conversely, the fractal nature of critical phenomena offers the possibility of realizing "fractals on fractals" (with two distinct dimensions) on these surfaces: Adlayer phase transitions (Section 4) and on-surface diffusion (random walks) are examples. Others may come from supported metal catalysts, say with silica gel or alumina as support, if the dispersed metal particles alone constitute a fractal (fractal dimension by fragmentation[8]) as one expects in certain cases. Work on these and other aspects is in progress.

ACKNOWLEDGMENTS

Helpful discussions with R. F. Fleming, G. Comsa, and H. Ibach on the proposed neutron experiment are acknowledged. Grants by the University of

Bielefeld and by the Ben-Gurion Fund, and assistance by the Fritz Haber Research Center for Molecular Dynamics (Jerusalem) are acknowledged.

REFERENCES

1. D. Avnir and P. Pfeifer, *Nouv. J. Chim.* **7**:71 (1983).
2. P. Pfeifer, D. Avnir, and D. Farin, *Surf. Sci.* **126**:569 (1983).
3. P. Pfeifer and D. Avnir, *J. Chem. Phys.* **79**:3558 (1983); **80**:4573 (1984).
4. D. Avnir, D. Farin, and P. Pfeifer, *J. Chem. Phys.* **79**:3566 (1983).
5. D. Avnir, D. Farin, and P. Pfeifer, *Nature* **308**:261 (1984).
6. P. Pfeifer, *Appl. Surf. Sci.* **18**:146 (1984).
7. D. Avnir, D. Farin, and P. Pfeifer, *J. Colloid Interface Sci.*, in press.
8. B. B. Mandelbrot, *The Fractal Geometry of Nature* (Freeman, San Francisco, 1982).
9. R. S. Sayles and T. R. Thomas, *Nature* **271**:431 (1978); M. V. Berry and J. H. Hannay, *Nature* **273**:573 (1978); P. A. Burrough, *Nature* **294**:240 (1981).
10. H. G. E. Hentschel and I. Procaccia, *Phys. Rev. A* **28**:417 (1983).
11. S. Lovejoy, *Science* **216**:185 (1982).
12. E. Jakeman, *Nature* **307**:110 (1984).
13. L. Niemeyer, L. Pietronero, and H. J. Wiesmann, *Phys. Rev. Lett.* **52**:1033 (1984).
14. D. Paumgartner, G. Losa, and E. R. Weibel, *J. Microscopy* **121**:51 (1981).
15. J. E. Avron and B. Simon, *Phys. Rev. Lett.* **46**:1166 (1981).
16. M. Suzuki, *Progr. Theor. Phys.* **69**:65 (1983).
17. A. Kapitulnik, A. Aharony, G. Deutscher, and D. Stauffer, *J. Phys. A* **16**:L269 (1983); D. C. Hong and H. E. Stanley, *J. Phys. A* **16**:L475 (1983), and references cited therein.
18. S. Havlin and D. Ben-Avraham, *Phys. Rev. A* **26**:1728 (1982).
19. I. Magid, Z. Djordjevic, and H. E. Stanley, *Phys. Rev. Lett.* **51**:143 (1983).
20. T. A. Witten and P. Meakin, *Phys. Rev. B* **28**:5632 (1983); H. Gould, F. Family, and H. E. Stanley, *Phys. Rev. Lett.* **51**:686 (1983); F. Family, *Phys. Rev. Lett.* **51**:2112 (1983); P. Meakin, *Phys. Rev. Lett.* **51**:1119 (1983); M. Kolb, R. Botet, and R. Jullien, *Phys. Rev. Lett.* **51**:1123 (1983).
21. P. Bak, *Rep. Progr. Phys.* **45**:587 (1982).
22. D. J. Thouless and Q. Niu, *J. Phys. A* **16**:1911 (1983); R. E. Prange, D. R. Grempel, and S. Fishman, *Phys. Rev. B* **28**:7370 (1983), and references cited therein.
23. D. Campbell and H. Rose, eds., *Order in Chaos*, *Physica* **7D** (1983), Chap. 4.
24. C. P. Allen, J. T. Colvin, D. G. Stinson, C. P. Flynn, and H. J. Stapleton, *Biophys. J.* **38**:299 (1982).
25. R. F. Voss, R. B. Laibowitz, and E. I. Allessandrini, *Phys. Rev. Lett.* **49**:1441 (1982); A. Kapitulnik and G. Deutscher, *Phys. Rev. Lett.* **49**:1444 (1982).
26. M. S. Wolfe, 57th Colloid and Surface Science Symposium, Toronto, 1983.
27. D. A. Weitz and M. Oliveria, preprint (1983).
28. B. H. Kaye, *Direct Characterization of Fineparticles* (Wiley, New York, 1981), Chapter 10.3; S. Peleg, J. Naor, R. Hartley, and D. Avnir, *IEEE Trans. Pattern Anal. Machine Intell.*, in press.
29. Y. Gefen, A. Aharony, and B. B. Mandelbrot, *J. Phys. A* **16**:1267 (1983); J. A. Given and B. B. Mandelbrot, *J. Phys. B* **16**:L565 (1983).
30. G. Binnig and H. Rohrer, *Helv. Phys. Acta* **55**:726 (1982).
31. A. W. Adamson, *Physical Chemistry of Surfaces*, 4th ed. (Wiley, New York, 1982); S. J. Gregg and K. S. W. Sing, *Adsorption, Surface Area, and Porosity*, 2nd ed. (Academic Press, London, 1982).

32. D. Farin, D. Avnir, and P. Pfeifer, *Langmuir* **1**, to appear.
33. U. Welz, H. Wippermann, and P. Pfeifer, unpublished.
34. P. G. Watson, in *Phase Transitions and Critical Phenomena*, Vol. 2, C. Domb and M. S. Green, eds. (Academic Press, London, 1972), p. 101.
35. Y. Gefen, B. B. Mandelbrot, and A. Aharony, *Phys. Rev. Lett.* **45**:855 (1980); Y. Gefen, Y. Meir, B. B. Mandelbrot, and A. Aharony, *Phys. Rev. Lett.* **50**:145 (1983); Y. Gefen, A. Aharony, and B. B. Mandelbrot *J. Phys. A* **16**:1267 (1983).
36. R. Jackson, *Transport in Porous Catalysts* (Elsevier, Amsterdam, 1977); R. E. Cunningham and R. J. J. Williams, *Diffusion in Gases and Porous Media* (Plenum Press, New York, 1980); E. A. Mason and A. P. Malinauskas, *Gas Transport in Porous Media: The Dusty-Gas Model* (Elsevier, Amsterdam, 1983).
37. R. J. Good and R. S. Mikhail, *Powder Technol.* **29**:53 (1981).
38. M. V. Berry, *J. Phys. A* **12**:781 (1979); M. V. Berry and T. M. Blackwell, *J. Phys. A* **14**:3101 (1981).
39. H. Steinhaus, *Coll. Math.* **3**:1 (1954).
40. P.-G. de Gennes, *C. R. Acad. Sci. Paris, Ser. II* **295**:1061 (1982).
41. A. Le Mehaute and G. Crepy, *C. R. Acad. Sci. Paris, Ser. II* **295**:685 (1982); A. Le Mehaute and G. Crepy, in *Fast Ion Transport in Solids* (North-Holland, Amsterdam, 1984) to appear.
42. F. H. Constable, *in Handbuch der Katalyse*, Vol. 5, G.-M. Schwab, ed. (Springer, Vienna, 1957), p. 141; D. Kalló, in *Contact Catalysis*, Vol. 1, Z. G. Szabó, ed. (Elsevier, Amsterdam, 1976), p. 306.
43. H. Kral, *Ber. Bunsen-Ges.* **75**:1114 (1971).